Cryogenic nanoindentation size effect in [0 0 1]-oriented face-centered cubic and body-centered cubic single crystals

Seok-Woo Lee, Lucas Meza, and Julia R. Greer

Citation: Appl. Phys. Lett. **103**, 101906 (2013); doi: 10.1063/1.4820585
View online: https://doi.org/10.1063/1.4820585
View Table of Contents: http://aip.scitation.org/toc/apl/103/10
Published by the American Institute of Physics

Cryogenic nanoindentation size effect in [0 0 1]-oriented face-centered cubic and body-centered cubic single crystals

Seok-Woo Lee,[a] Lucas Meza, and Julia R. Greer
Division of Engineering and Applied Science, California Institute of Technology, 1200 E California Blvd, Pasadena, California 91125, USA

(Received 11 April 2013; accepted 20 August 2013; published online 6 September 2013)

Cryogenic nanoindentation experiments performed on [0 0 1]-oriented single crystalline Nb, W, Al, and Au in an *in situ* nanomechanical instrument with customized cryogenic testing capability revealed temperature dependence on nanoindentation size effect. The Nix-Gao model, commonly used to capture indentation size effect at room temperature, does not take into account thermal effects and hence is not able to explain these experimental results where both hardness at infinite indentation depth and characteristic material length scale were found to be strong functions of temperature. Physical attributes are critically examined in the framework of intrinsic lattice resistance and dislocation cross-slip probability. [http://dx.doi.org/10.1063/1.4820585]

Nanoindentation has been widely used as a depth-sensing technique to measure the hardness and the elastic modulus of materials,[1,2] and it is common to observe an indentation size effect (ISE), where the hardness of crystalline materials increases at shallower indentation depths.[3,4] The Nix-Gao model explains the rise in hardness at lower indentation depths by linking it to the higher density of the geometrically necessary dislocations (GNDs), but it does not take into account the physical processes like dislocation interactions and cross-slip.[5–7] It is natural for the deformed volume under the nanoindenter tip to contain a high density of dislocations, on the order of $10^{14} \sim 10^{16}\,\mathrm{m}^{-2}$, which interact with one another through a number of complex mechanisms. The effects of such dislocation interactions on the mechanical properties obtained via nanoindentation would be obscured at a single temperature, but would emerge at different temperatures because dislocation interactions is often thermally activated and facilitated. For instance, the annihilation of screw dislocation dipoles caused by their thermally activated cross slipping directly affects the storage of dislocations in cold-rolling and dynamic recovery during stage III hardening.[8,9] The role of thermally activated cross-slip processes has never been carefully studied for ISE, where this mechanism is expected to be prevalent in the material volume directly underneath of the indenter. Thus, it should be worthwhile to elucidate the relation between thermally activated processes and ISE with the temperature control capability.

Mechanical properties of solids at low temperatures need to be carefully studied to ensure reliable functioning of structures, especially in space, where the environment is often cryogenic. Thus, we developed a capability to conduct nanomechanical experiments at cryogenic temperatures in a custom-built *in situ* instrument, InSEM^{TM} (Nanomechanics, Inc.).[10] The details of our customized instrumental system are provided in supplementary material.[11] Using this cryogenic setup, we performed nanoindentation experiments on two body-centered cubic (bcc), W and Nb, and two face-centered cubic (fcc), Al and Au, all oriented along [0 0 1] crystallographic direction. Prior to the mechanical experiments, Nb and W samples were electro-polished, and Al and Au were mechanically polished. Samples were indented at a constant loading rate of 4 mN/s to four different maximum loads, 4, 12, 20, and 28 mN and at the three different temperatures at 298 K, 230 K, and 160 K. Thermal drift was reduced to 0.5–4 nm/s by simultaneous cooling of the sample and of the indenter tip by the cold connection from the cold finger (Janis Research Company). Minimizing thermal drift during nanoindentation experiments is critical to ensure an accurate displacement measurement; the calculated error in displacement in the experiments presented here was less than ~5%. Indenter area function was calibrated using the Oliver-Pharr method.[2] No noticeable pile-up or sink-in was observed during *in situ* nanoindentation. Also, measurable pop-in in our experiments was not observed. Pop-in is typically related to initial microstructure and tip bluntness.[12,13] We confirmed that the more blunt tip produces measurable pop-in on the same W sample. Thus, the tip sharpness is an important factor to produce pop-in displacement. Also, our *in situ* system has relatively high machine vibrations of $10 \sim 30$ nm, which could make the system miss the small pop-in under the low load.

Figures 1(a) and 1(b) show a photograph of InSEM with the cryogenic set-up and a snapshot of a nanoindentation on Nb at 160 K. Figure 1(c) shows the configuration of cryogenic system. Figure 2 displays the load-displacement data during indentation into Nb, W, Al, and Au, and shows that for a given maximum load, the maximum displacement decreased at lower temperatures, which led to the increased hardness. For hardness calculation, the contact depth was obtained quasi-statically by the least squares fitting of the unloading data between 75% and 90% of the maximum load. The data of $(H/H_0)^2$ vs. $1/h$ for each metal at three different

[a]Author to whom correspondence should be addressed. Electronic mail: swlee49@caltech.edu

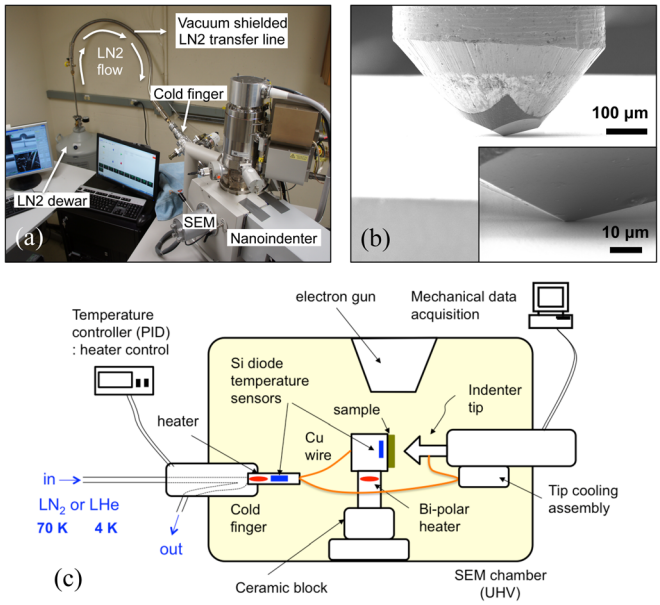

FIG. 1. (a) The cryogenic *in situ* mechanical testing set up, (b) the captured *in situ* SEM image of nanoindentation on Nb at 160 K, and (c) the schematic diagram of configuration of cryogenic system.

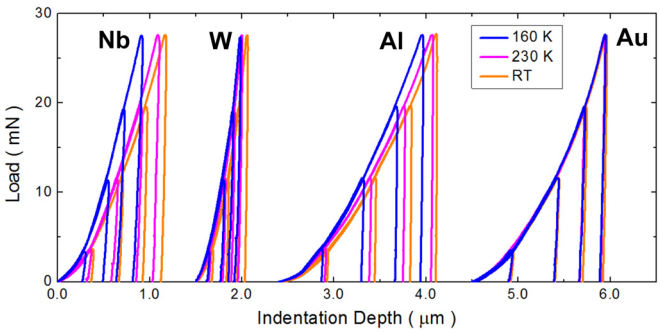

FIG. 2. Load-displacement curves of Nb, W, Al, and Au at 298 K (RT), 230 K, and 160 K with 4, 12, 20, and 28 mN of the maximum loads.

temperatures are plotted in Fig. 3 and appear to be linearly correlated.

Mechanical properties of crystals vary with the intrinsic lattice resistance, which increases at lower temperatures, especially in bcc crystals.[14,15] Qiu *et al.*[15] incorporated the effect of the intrinsic lattice resistance into the original Nix-Gao model, and quantified it in the following expression for hardness as a function of indentation depth:

$$\frac{H}{H_0} = \frac{3\sqrt{3}\tau_0}{H_0} + \sqrt{\left(1 - \frac{3\sqrt{3}\tau_0}{H_0}\right)^2 + \frac{h^*}{h}}, \quad (1)$$

where τ_0 is the intrinsic lattice resistance and all other parameters follow the nomenclature of the Nix-Gao formulation. They demonstrated that Eq. (1) maintains the approximately linear relation between $1/h$ and $(H/H_0)^2$ even for W, which has the highest intrinsic lattice resistance in this study. Thus, a reasonable representation of Eq. (1) might be

$$\frac{H}{H_0} = \frac{3\sqrt{3}\tau_0}{H_0} + \sqrt{\left(1 - \frac{3\sqrt{3}\tau_0}{H_0}\right)^2 + \frac{h^*}{h}} \approx \sqrt{1 + \frac{h^*_{eff}}{h}}, \quad (2)$$

where h^*_{eff} is the slope of $(H/H_0)^2$ vs. $1/h$ with the intrinsic lattice resistance taken into account. This approximation is consistent with the data shown in Fig. 3, where experimentally determined $(H/H_0)^2$ are plotted as a function of $1/h$ for each material and exhibit linear scaling. All h^*_{eff} and H_0 values at 160, 230, and 298 K are tabulated at Table I. This close-to-linear relation of hardness with h^*_{eff} is different from that in the original formulation of the Nix-Gao model for h^* because h^*_{eff} contains the effect of $3\sqrt{3}\tau_0/H_0$. However, Qiu *et al.* showed that this form of h^*_{eff}'s inverse dependence on H_0 is similar to that in the Nix-Gao model for h^*

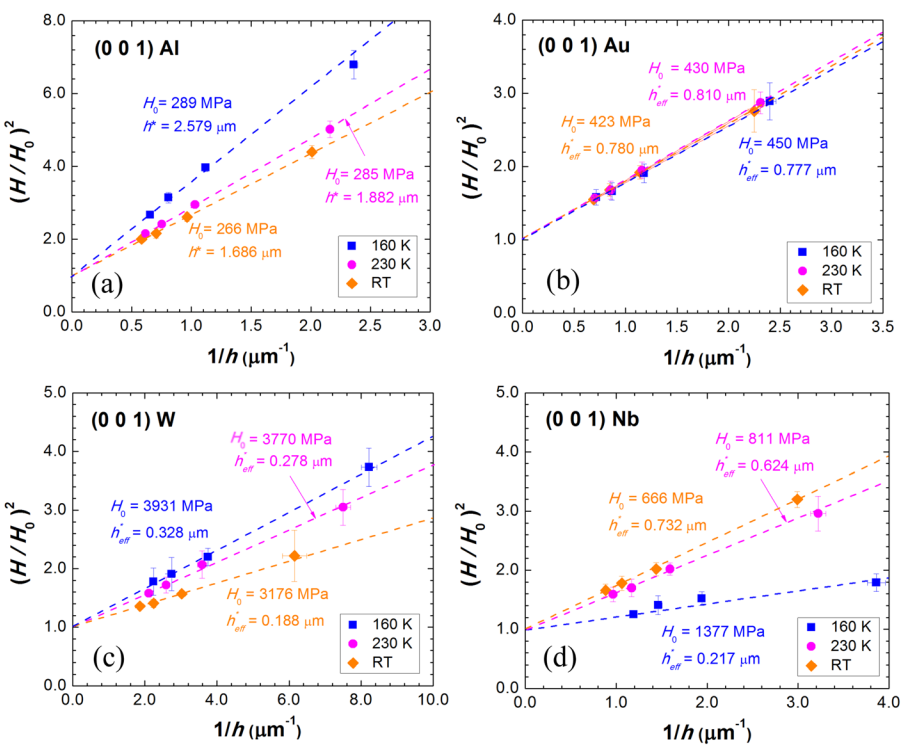

FIG. 3. Normalized hardness, $(H/H_0)^2$ as a function of the inverse indentation depth, $1/h$ for (a) Al, (b) Au, (c) W, and (d) Nb at 298 K (RT), 230 K, and 160 K.

TABLE I. h^*_{eff} and H_0 values at 160, 230, and 298 K.

	Al		Au		W		Nb	
T (K)	h^*_{eff} (μm^{-1})	H_0 (GPa)	h^*_{eff} (μm^{-1})	H_0 (GPa)	h^*_{eff} (μm^{-1})	H_0 (GPa)	h^*_{eff} (μm^{-1})	H_0 (GPa)
160	2.579	289	0.810	450	0.328	3931	0.217	1377
230	1.882	285	0.777	430	0.278	3770	0.624	811
298	1.686	266	0.780	423	0.188	3176	0.732	666

$$h^* = (81/2)b\alpha^2 \tan^2\theta(\mu/H_0)^2. \quad (3)$$

Here, α is the Taylor coefficient, μ is the shear modulus, b is the magnitude of the Burgers vector, and θ is the angle between the conical indenter tip and the sample surface.[3]

H_0 and h^*_{eff} in Eq. (2) represent two important physical quantities. H_0 is defined as $H_0 = 3\sqrt{3}(\tau_0 + \alpha\mu b\sqrt{\rho_{SSD}})$, where ρ_{SSD} is the density of statistically stored dislocations (SSDs), which is associated with the average strain.[3,15] Generally, the intrinsic lattice resistance, τ_0, in bcc crystals increases at lower temperatures[15] and enhances the hardness, H_0. Table I shows that the dependence of H_0 on temperature for Al and Au was relatively weak, but was more pronounced for Nb and W. The absolute change in H_0 between 298 K and 160 K was similar for both metals (W: 755 MPa and Nb: 711 MPa), but the relative change in H_0 was a factor of ~5 higher for Nb (W: 24% and Nb: 107 Nb %). This implies that Nb has a stronger temperature dependence of intrinsic lattice resistance, consistent with the previous observations in uniaxial tensile tests on Nb and W at ~190 K.[16,17]

The dependence of the physical parameter, h^*_{eff}, on temperature is less intuitive. The model of Qiu *et al.* implies that an increase in H_0 always leads to a lower h^*_{eff}.[15] The experimental results in Fig. 4 show that this was true for Nb but not for Au, which exhibited no noticeable temperature dependence of h^*_{eff}. For W and Al, both showed the opposite trend, and a similar experimental finding of higher h^*_{eff} at lower temperatures was recently reported in high-temperature nanoindentation on Cu.[18] This Cu work mentioned the temperature-dependent storage volume for the GNDs to explain their temperature effects.[18–20] The size of the plastic zone as well as the storage volume could be affected by dislocation mechanisms, which could be different with material parameter and temperature. However, the model of Qui *et al.* assumes the storage volume of GNDs as the hemisphere volume with the tip contact radius for all materials, as the Nix-Gao model does. According to Durst *et al.*, the plastic zone size is relatively similar for different materials at room temperature.[20] However, at a different temperature, the plastic zone size could be material-dependent. In an experimental way, it is not easy to distinguish between the change in dislocation structure and the change in the storage volume. For example, the decrease in dislocation density, which causes the decrease in hardness, could occur by either the dislocation annihilation or the increase in the storage volume of GNDs. For the better clarification, an advanced computational technique, such as dislocation dynamics simulation, would be necessary. In Cu work,[18] it was argued that the higher dislocation mobility at the higher temperature leads to the larger GND storage volume. However, our results show the completely opposite trend between W and Nb regardless of the similar temperature effects on the dislocation mobility. This indicates that there exists another dislocation mechanism to explain the temperature effects on the ISE.

According to the Nix-Gao, there are two contributions of dislocation density: one is the depth-independent part of dislocation density, and the other is the depth-dependent part of dislocation density. The Nix-Gao model assumes that the latter is the GND density, but here we would like to use the more generic meaning, the depth-dependent part of dislocation density, which can be expressed as

$$\rho_{depth-dependent}(h,T) = \frac{1}{27\alpha^2\mu^2b^2} \times \frac{H_0^2(T) \times h^*(T)}{h}, \quad (4)$$

for materials with low intrinsic lattice resistance ($\tau_0 \approx 0$). In this study, Al and Au represent the materials class with low lattice resistance, $\tau_0 \approx 0$ and $h^* \approx h^*_{eff}$. Equation (4) implies that h^* must depend on the $\rho_{depth-dependent}$ and hence, on temperature, because H_0 is relatively temperature-insensitive for fcc crystals. Figures 5(a) and 5(b) show $\rho_{depth-dependent}$ as a function of h at each temperature for Al and Au. These plots

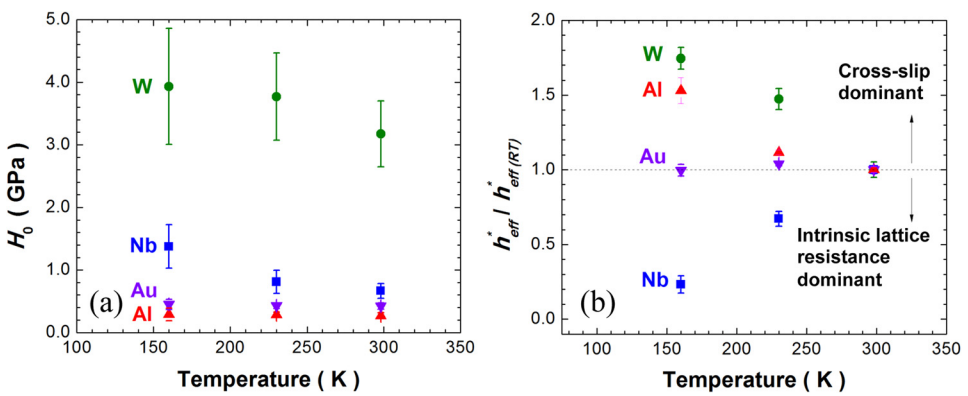

FIG. 4. (a) H_0 vs. temperature and (b) $h^*_{eff}/h^*_{eff(RT)}$ vs. temperature for the 4 metals studied. $h^*_{eff(RT)}$ is the characteristic length scale at room temperature (298 K).

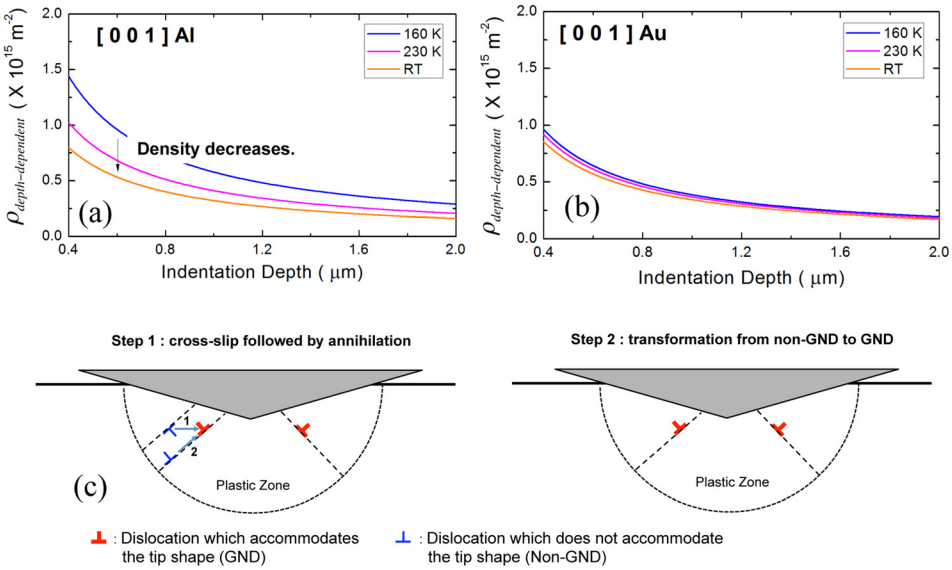

FIG. 5. Density of GND calculated by Eq. (4) as a function of indentation depth for each temperature for (a) Al and (b) Au. Fig. 4(c) shows schematic representation of dislocation annihilation mechanism (step 1) during nanoindentation. Note that both types of dislocations are distributed depth-dependently throughout the deformed crystal volume but only the GND contribute to the tip shape accommodation.

reveal that $\rho_{depth-dependent}$ decreases more rapidly in Al as compared with Au as the temperature increases: for the indentation depth of 500 nm, the change in $\rho_{depth-dependent}$ between 160 K and RT in Al is ~50% while that in Au is only ~10%. This is likely a result of more frequent dislocation annihilation events in Al, whose narrow stacking fault width enables the screw dislocations with compact cores to have a high probability for cross-slip. Note that our Al and Au samples were mechanically polished. Mechanical polishing usually makes the ISE more significant compared to electropolishing.[20,21] Then, the temperature effects on the ISE would also be exaggerated since the higher SSD density near the surface could cause more prolific mechanical recovery at the swallow indentation depth. However, both Al and Au samples in this study were prepared in the exactly same way, and the distribution of SSDs would be nominally similar. Thus, the clear difference in Figs. 3(a) and 3(b) still demonstrates the importance of cross-slip process during nanoindentation.

Figure 3(c) shows that h^*_{eff} decreases with temperature in W, as does in Al. In our previous nanopillar studies, uniaxial tension experiments on single crystalline W and Nb nanopillars showed that cross-slip was more prevalent in W than in Nb.[22] Post-deformation SEM images in this work clearly show that the slip traces in W were wavy, without significant shear offsets; in contrast to Nb, whose deformation was characterized by well-defined and straight shear offsets. The similar deformation behavior were also observed in larger micropillars.[23] These observations are consistent with the high room-temperature intrinsic lattice resistance reported for W, 344 ~ 370 MPa and an insignificant one for Nb, 14 ~ 27 MPa.[24] In metals with a high intrinsic lattice resistance, the fraction of screw dislocations is higher than that of the edge components under the applied stress because of the low mobility of screw dislocations, leading to more frequent cross-slip events. The high cross-slip probability in Al and W in this study may help explain a similar trend in the temperature-dependent ISE (Figs. 2(a) and 2(c)). The annihilation of screw dislocation dipoles as a result of cross-slip processes has been reported to limit the dislocation storage during severe plastic deformation.[8,9]

In fact, the Nix-Gao model does not take into account this dislocation annihilation process. The Nix-Gao model assumes that (1) the GND density is constant for a given indentation depth, and (2) that all of the dislocations that has a depth-dependent ($1/h$ dependence) distribution in the deformed volume are geometrically necessary. These two assumptions need to be assessed carefully to explain our observation in temperature effect on the ISE. The first assumption may not hold true when thermal effects are taken into account. For example, cold rolling of aluminum commonly generates very high dislocation densities, $\sim 10^{14}\,m^{-2}$ but high temperature-rolled aluminum has the low dislocation density due to dynamic recovery, i.e., dislocation annihilation, even under the nominally similar applied strains.[25,26] At higher temperatures, the existing dislocation structures are able to evolve into lower energy configurations with reduced dislocation and strain energy densities while keeping the net Burgers vector. The 2nd assumption also represents an idealized case. Zaiser and Aifantis pointed out that there is no reason for all of the dislocations that has the depth-dependent distribution within the deforming volume to be GNDs.[6] Additional dislocations may be nucleated from the surface as prismatic loops or as glide dislocations,[27] and the pre-existing SSDs can be transformed into GNDs, forming complex dislocation networks throughout the volume.[5,7] Thus, Eq. (4) need not be restricted to the GND-only density and should include some dislocations, which do not necessarily contribute to the accommodation of the tip shape. That was why we used $\rho_{depth-dependent}$ rather than ρ_{GND} in Eq. (4). Figure 5(c) shows a schematic representation of the dislocation annihilation mechanism during nanoindentation. Here, the thick (red color) symbols represent the GNDs, which accommodate the indenter tip shape. The thin (blue color) symbols represent the remaining dislocations that do not contribute to the shape change. Both types of dislocations have depth-dependent distribution. So, they are included in the dislocation density in Eq. (4). Step 1 corresponds to the annihilation of two oppositely signed screw dislocations by cross-slip and step 2 corresponds to a non-GND-to-GND transformation of a dislocation to satisfy the boundary conditions. The remaining dislocations, which are not shown in

Fig. 4(c), would also have to slightly re-arrange themselves to accommodate the *exact* tip shape change. The consequence of this process is dislocation annihilation (step 1) followed by dislocation character change (step 2) is a lower dislocation density in the deformed volume and a smaller h^*_{eff} (or h^*) in Eq. (4) while keeping the permanent shape change.

In this phenomenological mechanism, metals that are amenable to dislocation cross-slip, W and Al in this study, would have a lower relative dislocation density within the indented volume compared with the hard-to-cross-slip metals, Nb and Au, at the same homologous temperature. This would be manifested by a lower h^*_{eff} in Eq. (4). At high temperatures, the dynamic recovery by dislocation annihilation is expected to be significant, which explains why the high temperature indentation on Cu in the work of Franke *et al.*[18] exhibits a similar trend as W and Al, but more pronounced temperature effect (~3.5 times increase in h^*_{eff} from 296 to 473 K). Because the cross-slip probability has an exponential dependence on temperature, the mechanical recovery rate would be more rapid at the higher temperature even though Cu (44.6 mJ/m^2) has the stacking fault energy lower than Al (145.5 mJ/m^2).[28]

In summary, we designed and constructed a cryogenic testing capability within the existing custom-made *in situ* nanomechanical instrument, InSEM. Using this setup, nanoindentation experiments were performed on single crystalline Nb, W, Al, and Au at 160, 230, and 298 K. Results indicate that the ISE manifested by a higher hardness, H, at the shallower indentation depths, h, holds for lower temperatures. The material hardness at infinite indentation depth, H_0, of the body-centered cubic metals, Nb and W, increased by 107% and 24%, respectively, but did not change significantly for the fcc samples, Al and Au, when the temperature was lowered from RT to 160 K. This can be explained by the amplification in the intrinsic lattice resistance with temperature reduction in bcc metals. The characteristic length scale term, h^*_{eff}, was found to depend on both the temperature and the material. We propose a physical deformation mechanism, based on dislocation cross-slip followed by dislocation annihilation and postulate it to be a key factor in determining h^*_{eff}. W and Al, had a high propensity for cross-slip and exhibited a similar relative increase in h^*_{eff}, on the order of 60%, as the temperature was reduced from RT to 160 K. Nb displayed the opposite trend, with h^*_{eff} decreasing by 80% over the same temperature range, likely because the increase in the intrinsic lattice resistance at low temperatures overrides the already-low probability for cross-slip. In Au, both H_0 and h^*_{eff} were virtually independent of temperature because of the temperature-insensitive dislocation mobility and the wide stacking fault width, resulting in a low cross-slip probability.

The authors gratefully acknowledge the financial support of the Kavli Nanoscience Institute (KNI) through SWL's prized post-doctoral fellowship and of the W. M. Keck Institute for Space Studies at Caltech. R. Maaß and R. Zmuidzinas are acknowledged for significant contributions in the initial instrumental design and preliminary data acquisition. W D. Nix is thanked for useful discussions.

[1]M. F. Doerner and W. D. Nix, J. Mater. Res. **1**, 601 (1986).
[2]W. C. Oliver and G. M. Pharr, J. Mater. Res. **7**, 1564 (1992).
[3]W. D. Nix and H. Gao, J. Mech. Phys. Solids **46**, 411 (1998).
[4]N. A. Fleck, G. M. Muller, M. F. Ashby, and J. W. Hutchinson, Acta Metall. Mater. **42**, 475 (1994).
[5]L. P. Kubin and A. Mortensen, Scr. Mater. **48**, 119 (2003).
[6]M. Zaiser and E. C. Aifantis, Scr. Mater. **48**, 133 (2003).
[7]G. M. Pharr, E. G. Herbert, and Y. Gao, Annu. Rev. Mater. Res. **40**, 271 (2010).
[8]A. Seeger, *Dislocations and Mechanical Properties of Crystals* (Wiley, New York, 1957), pp. 243–329
[9]U. F. Kocks, J. Eng. Mater. Technol. **98**, 76 (1976).
[10]J. R. Greer, J.-Y. Kim, and M. J. Burek, JOM **61**, 19 (2009).
[11]See supplementary material at http://dx.doi.org/10.1063/1.4820585 for the description of the customized cryogenic nanomechanical tester.
[12]S. Shim, H. Bei, E. P. George, and G. M. Pharr, Scr. Mater. **59**, 1095 (2008).
[13]S. K. Lawrence, D. F. Bahr, and H. M. Zbib, J. Mater. Res. **27**, 3058 (2012).
[14]D. Hull and D. J. Bacon, *Introduction to Dislocations* (Butterworth-Heinemann, Elsevier, Oxford, 2000).
[15]X. Qiu, Y. Huang, W. D. Nix, K. C. Hwang, and H. Gao, Acta Mater. **49**, 3949 (2001).
[16]H. C. Kim and P. L. Pratt, Mater. Res. Bull. **2**, 323 (1967).
[17]A. S. Argon and S. R. Maloof, Acta Metall. **14**, 1449 (1966).
[18]O. Franke, J. C. Trenkle, and C. A. Schuh, J. Mater. Res. **25**, 1225 (2010).
[19]G. Feng and W. D. Nix, Scr. Mater. **51**, 599 (2004).
[20]K. Durst, B. Backes, and M. Göken, Scr. Mater. **52**, 1093 (2005).
[21]Y. Lin and A. H. N. Ngan, Scr. Mater. **44**, 237 (2001).
[22]Y. Kim, D. Jang, and J. R. Greer, Acta Mater. **58**, 2355 (2010).
[23]A. S. Schneider, D. Kaufmann, B. G. Clark, C. P. Frick, P. A. Gruber, R. Mönig, O. Kraft, and E. Arzt, Phys. Rev. Lett. **103**, 105501 (2009).
[24]S.-W. Lee and W. D. Nix, Philos. Mag. **92**, 1238 (2012).
[25]C. C. Merriman, D. P. Field, and P. Trivedi, Mater. Sci. Eng., A **494**, 28 (2008).
[26]G. E. Totten and D. S. MacKenzie, *Handbook of Aluminum: Physical Metallurgy and Processes* (Marcel Dekker, Inc., 2003).
[27]J. Li, K. J. Van Vliet, T. Zhu, S. Yip, and S. Suresh, Nature **418**, 307 (2002).
[28]A. T. Jennings, C. R. Weinberger, S.-W. Lee, Z. H. Aitken, L. Meza, and J. R. Greer, Acta Mater. **61**, 2244 (2013).